3D reconstruction of existing concrete bridges using optical methods

Cosmin Popescu, Björn Täljsten, Thomas Blanksvärd & Lennart Elfgren

Published online: 13 Apr 2019.

Submit your article to this journal ↗

View Crossmark data ↗

 OPEN ACCESS Check for updates

3D reconstruction of existing concrete bridges using optical methods

Cosmin Popescu[a,b] , Björn Täljsten[a], Thomas Blanksvärd[a] and Lennart Elfgren[a]

[a]Deptartment of Civil, Environmental and Natural Resources Engineering, Luleå University of Technology, Luleå, Sweden; [b]Northern Research Institute—NORUT, Narvik, Norway

ABSTRACT
Routine bridge inspections usually consist of visual observations. These inspections are time-consuming and subjective. There is a need to identify new inspection techniques for infrastructure that reduce traffic disturbance, and improve the efficiency and reliability of the acquired data. This study compared the performance of three different imaging technologies for the three-dimensional (3D) geometric modeling of existing structures: terrestrial laser scanning, close-range photogrammetry, and infrared scanning. Each technology was used to assess six existing concrete railway bridges. The technologies were compared in terms of geometric deviations, visualization capabilities, the level of the inspector's experience, and degree of automation. The results suggest that all methods investigated can be used to create 3D models, however, with different level of completeness. Measurements such as span length, deck widths, etc. can be extracted with good accuracy. Although promising, a full off-site inspection is currently not feasible as some areas of the bridges were difficult to capture mainly due to restricted access and narrow spaces. Measurements based on terrestrial laser scanning were closer to the reality compared to photogrammetry and infrared scanning. The study indicates the no special training is needed for photogrammetry and infrared scanning to generate a 3D geometric model.

1. Introduction

Train timetables are made on the assumption that the necessary infrastructure always functions at the required level and is available for use. In reality however, disruptions to train services are becoming increasingly common as a result of scheduled maintenance work, visual inspections, and so on. Regular inspections of existing bridges are usually scheduled during their service life to evaluate their health and as part of a proactive maintenance regime in cases where deterioration is anticipated. Routine inspections typically consist of field measurements and visual observations made by a bridge inspector. Their main purpose is to gather information about issues such as concrete deterioration, steel rebar corrosion, water seepage, concrete cover delamination, spalling, deflection/settlements, cracks, and geometry (Alani, Aboutalebi, & Kilic, 2014; Phares et al. 2004; Riveiro & Solla, 2016).

The measurements and observations are typically documented in the form of field inspection notes, freehand sketches, and photographs which are then used as inputs in transportation agencies' bridge management protocols. The procedure is highly dependent on the inspector's experience (Phares et al., 2004), and knowledge of the structural behavior and material properties of the system being investigated. The method is limited in that only the accessible parts of the bridge can be investigated due to the difficult terrain in which the structure is sometimes located. This is especially true for large structures, such as bridges, where investigating the whole area would be very time-consuming and potentially unsafe (Abu Dabous et al. 2017).

In addition, defects can only be detected when their presence has become visible to the naked eye, at which point they may already have affected the life of the structure. Furthermore, knowledge transfer from one inspection period to another becomes difficult when successive investigations are performed by different inspectors. Graybeal et al. (2002) noted that routine inspections have relatively poor accuracy, with the following factors affecting the reliability of these results: the inspector's fear of traffic, near visual acuity, and color vision, as well as the accessibility and complexity of the structure. In addition, traffic volumes have increased considerably, meaning that track/road possession must be minimised (Hugenschmidt, 2002). Therefore, there is a strong need for new infrastructure inspection and monitoring techniques that reduce disruption and improve the efficiency and reliability of the acquired data.

2. Background

The use of emerging technologies in civil engineering is increasing rapidly. This is particularly true for optical methods—advanced alternatives to visual inspection in which objects are imaged using high precision, high sensitivity cameras. According to Fathi and Brilakis (2011), optical sensors can be classified as being active or passive. Active

sensors obtain depth information by emitting energy and recording the reflected signals; techniques using active sensors include terrestrial laser scanning (TLS), infrared scanning (IS), and imaging with Red-Green-Blue-Depth (RGB-D) cameras. Passive sensors use ambient light to capture details of the surrounding environment; the resulting images can then be post-processed to generate range data. A notable technique using passive sensors is close-range photogrammetry (CRP). The main output of such methods is a *point cloud*, which is considered to be the most primitive type of three-dimensional (3D) model that allows 3D measurements and drawings (Riveiro & Solla, 2016). Conde et al. (2017) used, among other non-destructive techniques, laser scanning to obtain all the necessary geometric data to build a detailed 3D finite element model of a masonry arch bridge. Stavroulaki et al. (2016) used laser scanning and photogrammetry to reduce the time needed to produce a realistic 3D geometric model of a masonry bridge. Jáuregui et al. (2009) showed that photogrammetry can be used to obtain measurements that would typically be acquired during routine inspections of a prestressed concrete bridge. Jáuregui et al. (2005) aimed at enhancing routine bridge inspections by turning still photographs into a 3D environment using QuickTime Virtual Reality.

Along with modeling of existing bridges, Chen et al. (2012) used TLS together and simple algorithms to retrieve damage information from geometric point cloud data. Terrestrial laser scanners have also been used to measure bridge clearance (Liu et al. 2012; Riveiro et al., 2013; Riveiro et al. 2012; Watson et al., 2012), bridge displacement during load testing (Liu et al., 2010), and to perform structural health assessments (Hess et al 2018).

Vaghefi et al. (2012) assessed 12 remote sensing technologies and their potential to detect various common problems in US bridges, concluding that 3D optical technologies have considerable potential for documenting surface-related defects. Similarly, Vaghefi et al. (2015) reported that a 3D optical bridge evaluation system (3DOBS) using inexpensive and easily deployable technology expedited inspection and visualization in a study on the quantification of defects in bridge deck surfaces.

Many studies have examined the use of unmanned aerial vehicles (UAV) for bridge inspection. The current status of UAVs for inspection purposes in infrastructure engineering was recently reviewed by Duque, Seo, and Wacker (2018), who highlighted reports showing that UAVs have successfully been used to detect damage such as cracks and corrosion. Consequently, transport agencies have already incorporated UAV-based methods into their existing bridge inspection and monitoring regimes. UAVs have also been used together with infrared thermography to detect subsurface delaminations in concrete bridge decks (Omar & Nehdi, 2017). This combined approach was found to yield results more quickly and with less labor than traditional nondestructive testing methods. Franco et al. (2017) used two RGB-D cameras (Kinect V1 and Kinect V2) to measure displacements during experimental tests of structural elements, achieving mean displacement errors of 3.4% and

7.9% for static and dynamic displacements, respectively. Displacement fields under dynamic loads were measured using an RGB-D camera (Kinect V1) by Abdelbarr et al. (2017). The tested sensor was found to be a low-cost solution capable of monitoring multi-component displacement with an error of less than 5% for displacements larger than 10 mm. Optical methods have also been used by Henry et al. (2014) for 3D modeling of indoor environments, and by (Takimoto et al., 2016) for 3D reconstruction of various objects. Jáuregui et al. (2003) reported that photogrammetry performed with semi-metric digital cameras has accuracy ranging from 2–10% of the measured vertical displacements. The study was performed on a laboratory-tested steel beam. The technique has also been tested on-site on a prestressed concrete bridge to measure the initial camber and dead load deflection. Photogrammetric results showed an average difference of about 3.2 mm as compared with measurements made with a total station (Jáuregui et al., 2003). Golparvar et al. (2011) used a 3D reconstruction approach in four construction projects and four laboratory settings and compared the outcome to results obtained with a laser scanner. The image-based approach was less accurate than laser scanning, but both techniques offered good visualization. Bhatla et al. (2012) used commercial photogrammetry software to model an under-construction bridge to evaluate its accuracy against as-built 2D drawings. Measured beam lengths and box girder heights were overestimated and underestimated by 2% and 5%, respectively. Although the authors discussed several challenges they encountered when using the imaging software (including occlusion by natural vegetation and the presence of water), they concluded that the optical method had potential for measuring dimensions in inaccessible zones, facilitating digital storage for visualization purposes, and improving decision-making, among other things (Bhatla et al., 2012). Riveiro et al. (2013) tested the accuracy of photogrammetry and laser scanning methods for measuring the vertical underclearance during bridge inspection. While the laser-scanning had better accuracy, the accuracy achieved using photogrammetry was in the range of ±2 cm. The photogrammetry was performed using photos captured with four different cameras having resolutions ranging from 6.3 to 21.1 megapixels. Better results were obtained with higher quality cameras. More recently, Khaloo et al. (2018) described the use of UAVs to produce 3D models with enough accuracy to detect defects on an 85m-long timber truss bridge. The UAV-based method was found to outperform laser scanning with respect to the quality of the captured point clouds, the local noise level, and the ability to render damaged connections.

3. Scope and scientific relevance

As can be seen, there have been many studies on the use of machine vision to inspect and monitor civil infrastructure. However, many of these studies were conducted under near-ideal conditions (e.g. in laboratory settings, in cases without natural vegetation surrounding the studied object, focusing on small-scale objects, and conducted by trained

Figure 1. Bridge locations and photos of the bridges taken on the day of scanning 'Map by Maphill'.

personnel and/or under favorable weather conditions). This study thus contributes to the literature by evaluating the performance of three optical methods (TLS, CRP, and IS) under nonideal conditions. The methods were evaluated with respect to accuracy, time-consumption, costs, and degree of automation.

In addition, the photogrammetry was performed by personnel with different levels of training. Team 1 (which performed photogrammetry and infrared scanning) consisted of two MSc students with no prior experience other than a few trials in a laboratory before the field trip, while Team 2 (which performed both photogrammetry and laser scanning) consisted of two experienced surveyors who carried out the scanning. Because the teams had different levels of experience and used different workflows and software, it was possible to compare their performance and the quality of their results. The study examined six concrete railway bridges spanning flowing water and traffic-carrying roads, located in both urban and rural areas. Most of them were surrounded by vegetation. Because of the long distances between the bridges, the surveys were carried out under severe time constraints, over a period of 5 days.

4. Field deployment

4.1. The selected bridges

The Swedish Transport Administration (Trafikverket) selected the bridges on which the technologies were to be tested. In total, six bridges located in northern Sweden along the Iron Ore Line were selected, all in service. Traffic flow was not disrupted at all during the survey. However, a safety representative informed the team whenever a train was about to arrive. The bridges' accessibility varied – some were readily accessible (e.g. a bridge crossing a road in a town), while others were not (e.g. a bridge in a remote area with rough terrain).

The study was carried out over a relatively short period of 5 days, including a half-day safety course and the time

needed to travel between the site locations (which involved approximately 1000 km of driving). Each site was visited prior to the experiment to perform a preliminary screening of the bridges, establish optimal scanning positions and locations, and secure access. Figure 1 presents photographs of the six bridges and their locations; the bridges are numbered in the order they were scanned.

4.2. Edbäcken bridge

Built in 1886 with the superstructure replaced in 1977, the Edbäcken bridge (Bridge 1 in Figure 1) is a simply supported reinforced concrete (RC) trough bridge with a span of 5.8 m and a width of 3.8 m. The bridge spans a stream with a maximum depth of 0.7 m and is surrounded by dense vegetation. Testing was carried out on a sunny day.

4.3. Påunakbäcken bridge

Built in 1887 with the superstructure replaced in 1998, the Påunakbäcken bridge (Bridge 2 in Figure 1) is a simply supported RC slab bridge with a span of 2.95 m and a width of 4.5 m. The bridge spans a 0.5 m deep stream. The surrounding area is wet and full of wild bushes and trees. Testing was carried out on a sunny day.

4.4. Kedkejokk bridge

Built in 1906, the Kedkejokk bridge (Bridge 3 in Figure 1) is a concrete arch bridge with a span of 4.0 m and a width of 41.2 m. The bridge spans a fast-flowing stream with a depth of approximately 0.5 m. However, there are narrow platforms for walking on below the bridge. Because the bridge is relatively long, the ambient light level was low. Testing was performed on a cloudy day.

Table 1. Summary of data collected.

Bridge	TLS Scanning positions	CRP					IS Scanning positions
		Camera stations	No. of photos	ISO	Aperture	Shutter speed (sec)	
Edbäcken bridge	10[a]	12	90	160	f/8	1/10–1/200	N/A[c]
Påunakbäcken bridge	11[a]	55	581	160	f/10	1/6–1/125	13
Kedkejokk bridge	15[b]	25	621	160	f/8	1/4–1/20	17
Juovajokk bridge	15[b]	45	737	160	f/8	1/6	22
Pahtajokk bridge	11[a]	32	397	160	f/8	1/13	21
Kallkällevägen bridge	11[a]	142	744	160	f/8	1/8–1/25	67

[a]Each scanning generating about 30–40 million points of data.
[b]Each scanning generating about 20 million points of data.
[c]Due to strong interference from ambient light none of the scans aligned correctly.

Figure 2. Data acquisition equipment. (a) Terrestrial laser scanning—RIEGL VZ-400, (b) CRP—Canon EOS 5D, (c) unmanned aerial vehicle—3DR Site scan and (d) infrared scanning—Matterport Pro2 3D.

4.5. Juovajokk bridge

Built in 1902 with the superstructure replaced in 1960, the Juovajokk bridge (Bridge 4 in Figure 1) is a simply supported trough bridge with a span of 5.5 m and a width of 3.8 m. The bridge spans a fast-flowing but shallow stream of water. The surrounding area is densely vegetated and there are steep slopes behind the abutments. Testing was carried out on a cloudy day.

4.6. Pahtajokk bridge

Built in 1902 with the superstructure replaced in 1963, the Pahtajokk bridge (Bridge 5 in Figure 1) is a simply supported trough bridge with a span of 6.9 m and a width of 3.9 m. The bridge spans a fast-flowing stream of water (0.5 m deep). The surrounding area is wet with few trees on one side of the bridge; on the other side, the view is obstructed by dense vegetation. A fence surrounds the bridge to restrict access to the railway, hindering access to the abutments. Testing was carried out on a cloudy day after a heavy snowfall.

In addition to the data collected by Team 1 (presented in Table 1 for CRP) Team 2 also carried out photogrammetry scanning (both ground-based and aerial) on Pahtajokk bridge. The camera settings were similar, with 450 photos taken with the handheld camera and another 221 by the drone.

4.7. Kallkällevägen bridge

Built in 1966, the Kallkällevägen bridge (Bridge 6 in Figure 1) is a three-span RC continuous girder bridge with spans of 9.2 + 14.5 + 9.2 m and a width of 4.54 m. The bridge spans a two-lane road. The bridge is located inside a town, so no vegetation is present and the bridge can be clearly viewed from all angles. Access is restricted by fences, which also cover the abutments. Testing was carried out on a cloudy day.

5. Geometric reconstruction: techniques and equipment

This section briefly summarises the methods and equipment used to recreate 3D models. Details of the settings and the processes used when scanning the bridges (with particular emphasis on any deviations from the general procedure presented in Sections 5.1–5.3) are given in Table 1.

5.1. Terrestrial laser scanning—TLS

In TLS, the structure's 3D geometry is obtained using light detection and ranging technology (LiDAR). The system works by emitting light and detecting its reflection to determine the distance to the object. The 3D models are created by stitching together multiple scans on a common coordinate system. The technique uses either time-of-flight or phase-based technology to record the x, y, z coordinates and intensity data of the objects. The approaches used most commonly in civil engineering applications are based on time-of-flight (Riveiro & Solla, 2016).

The equipment used in this study was a long-range, RIEGL VZ-400, 3D terrestrial laser scanner (Figure 2(a)). This 3D scanner operates on the time-of-flight principle and can make measurements ranging from 1.5 m to 600 m with a nominal accuracy of 5 mm at 100 m range. It uses near-infrared laser wavelengths with a laser beam divergence of 0.3 mrad, corresponding to an increase of 30 mm of beam diameter per 100 m distance. The instrument's maximum
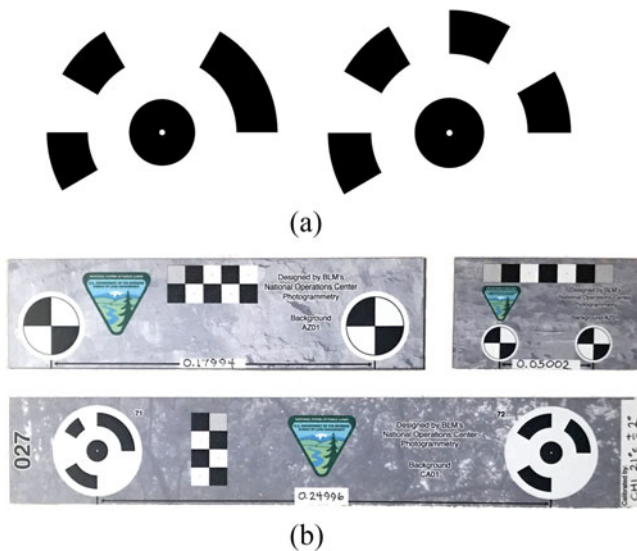
Figure 3. Artificial targets used in the alignment process and for scaling: (a) coded targets and (b) calibration scale bars.

vertical and horizontal scan angle ranges are 100° and 360°, respectively. The raw TLS data, i.e. point clouds captured from multiple scans, were post-processed (registered and geo-referenced) using the Leica Cyclone software package, which automatically aligns the scans and exports the point cloud in various formats for further processing.

5.2. Close-range photogrammetry—CRP

In CRP, a series of images is recorded using digital cameras, and coordinates of points (targets), patterns, and features in the images are subsequently identified using image processing techniques (Baqersad, Poozesh, Niezrecki, & Avitabile, 2017). The process of estimating the 3D structure of a scene from a set of two-dimensional (2D) images is known as structure from motion (SfM). The SfM approach was initially developed by the computer vision community to obtain structural information and estimate camera position based on multiple images (Fritsch & Klein, 2018). The approach relies on pixel correspondence between images and, unlike older photogrammetry algorithms, no pre-calibration of the camera is necessary. To make the process easier, the surfaces of the imaging object should have distinct features, either natural (e.g. sharp edges, discoloration, bolts, or rails) or artificial targets (see Figure 3). A minimum of 60% overlap between images is necessary, in both the longitudinal and transversal directions.

A commercial SfM software package, Agisoft PhotoScan Pro (LLC, 2017), was used to create 3D models by estimating the interior orientation and defining the orientation of the camera position for each photo relative to the scanned object. After processing the data, the software returns the camera positions and internal geometry of the camera from the calibration process. An example of its output is shown in Figure 4, which presents the camera stations used when imaging the Påunakbäcken bridge. The resulting 3D model generally lacks a scale, so a scale is added by the SfM algorithm in two different ways: (1) by adding known distances within the model, e.g. the distance between the artificial targets, or (2) by adding calibrated scale bars of known dimensions onto the scene. In this study, 12-bit coded targets (Figure 2(a)) were attached to the bridges at known distances measured on-site using a laser rangefinder.

The equipment (Figure 2(b)) consisted of a Canon EOS 5 D digital single-lens reflex (DSLR) camera with a full-frame (35.8 × 23.9 mm) complementary metal–oxide–semiconductor (CMOS) optical sensor giving a resolution of 12.8 megapixels (4368 × 2912 pixels). The camera was equipped with a Canon EF 35 mm wide-angle prime (fixed zoom) lens. On a full-frame camera body, this lens gives a large field of view (achieving a 54° horizontal viewing angle) covering a wide area, meaning that fewer images are needed to capture an entire structure.

For one of the bridges scanned, another team carried out additional photogrammetric scanning using a better camera (Canon EOS 5D Mark II) with a resolution of 21.1 megapixels and a Canon EF 24 mm prime lens. The images taken by the Canon EOS 5D Mark II were supplemented with aerial photos taken using a 3DR Site Scan drone equipped with a Sony R10C camera with a 16–50 mm zoom lens (Figure 2(c)). The Sony camera has a resolution of 20.1 megapixels and uses an APS-C size sensor. 3D models were generated using a commercial SfM software package—Bentley ContextCapture (Bentley, 2018).

Established best practices (Cultural Heritage Imaging, 2018) recommend that cameras should be configured as follows: (1) the aperture should remain fixed during the capture sequence (preferably not smaller than *f*/11 on a 35 mm camera to avoid diffraction effects); (2) the lowest possible ISO setting should be used; (3) image stabilization and auto-rotate camera functions should be disabled; and (4) in variable light conditions, the camera should be set to aperture priority mode (with the *f*-stop ranging from 5.6 to 11), which locks the aperture and evens out exposure by varying the shutter speed. These recommendations were followed as closely as possible; where deviations were necessary because of some peculiarity of a particular bridge, they are noted in Table 1.

5.3. Infrared scanning—IS

Infrared scanning uses RGB-D cameras in combination with an infrared camera and an infrared projector to augment the still image with depth information (Miranda & Abreu, 2016). The sensors project a structured infrared light pattern onto the scene, and the reflected light is captured by the infrared camera and used to calculate depths (Weinmann, 2016). The camera used in this study was a Matterport Pro2 3D Camera (Figure 2(d)) that has three infrared sensors for capturing depth data together with visual data (RGB) at 360° (left – right) and 300° (vertical). The images are captured at a resolution of 8092 × 4552 pixels.

The camera is wirelessly connected to a tablet from which the scanning is performed. The capture time for each scan is about 40 secs, including the transfer time from camera to tablet and the time needed for alignment. The camera's range is about 4.5 m in indoor environments. Although
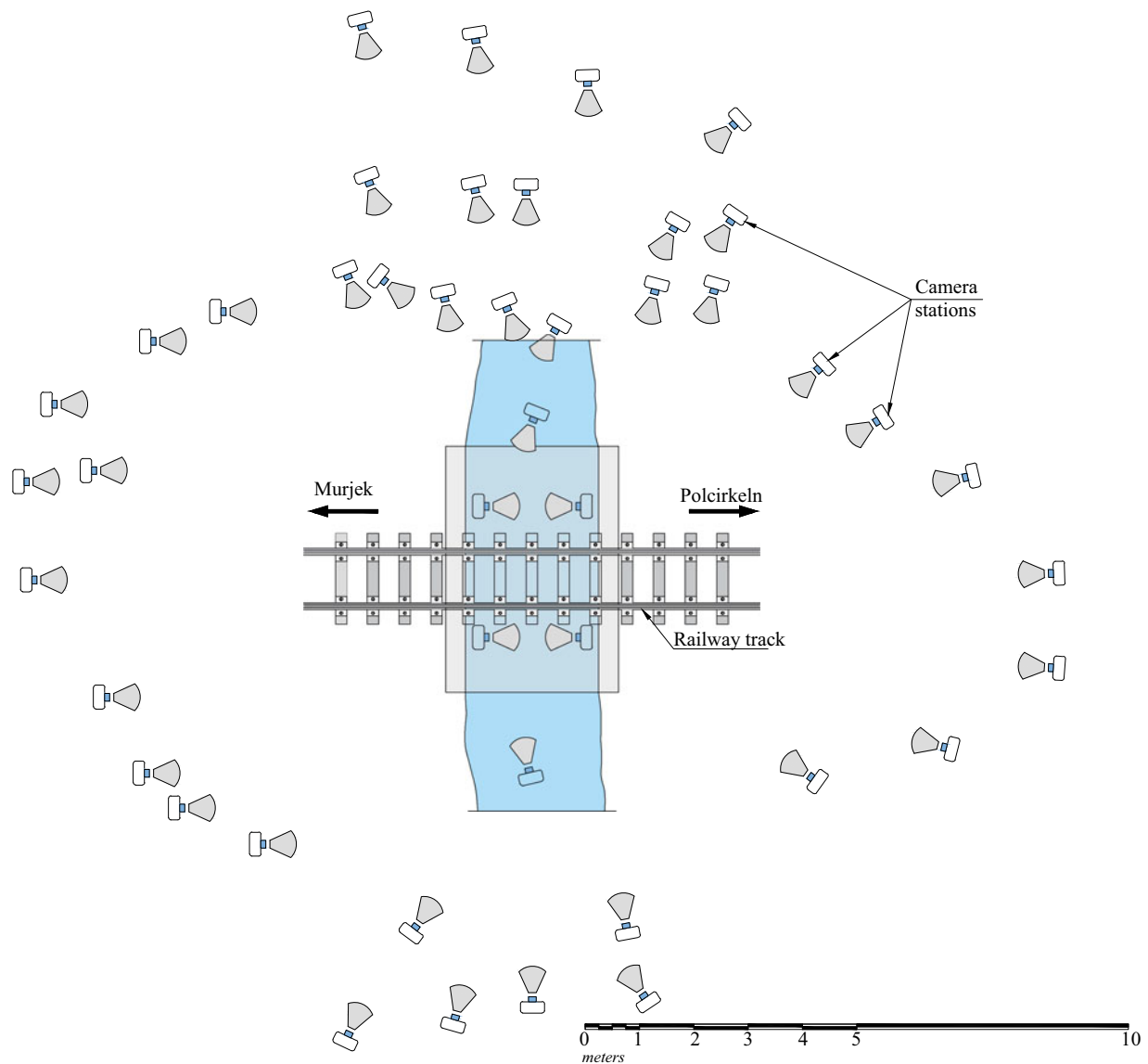
Figure 4. Different viewpoints and the resulting camera position triangulation of Påunakbäcken (modified from Agisoft PhotoScan Pro).

not supported by the developer, if scanning is performed outdoors, more scan positions are required. To avoid alignment issues, the scanning must be performed during civil twilight (30 minutes before sunrise or 30 minutes after sunset), or on a cloudy day to avoid infrared light from the sun. When completed, the scans are uploaded to Matterport's cloud service for 3D data registration and the point cloud is obtained. In addition, the scan positions around the bridge can be visualised, as shown for the Juovajokk bridge in Figure 5.

6. Results and discussion

Both quantitative and qualitative analyses were performed. The first step was to create a 3D model of each scanned bridge and compare the visual capabilities of each method. To perform visual inspections off-site, bridge inspectors require 3D models that are detailed enough to identify certain defects. A qualitative analysis was conducted to assess the potential of each of the three methods. Quantitative assessments were performed by calculating geometric

deviations with respect to the span length and width of each bridge deck.

6.1. Documentation and visualization

The first step to investigate was the visualization of the digital models including the level of detail captured by each optical method. The 3D models of each bridge generated by TLS, CRP and IS, are shown in Figures 6–10. Due to insufficient overlap between the photos, the Edbäcken bridge, which was the first to be scanned, could not be reconstructed. Alignment issues also occurred for the Matterport camera due to intense ambient light. Consequently, the only model for this bridge that could be created used laser-scanning data. However, because the objective of this work was to compare the potential of the three methods, the laser scanning-based 3D model is not shown.

For the remaining five bridges, sufficient photos were taken to provide adequate overlap for photogrammetry. Complete 3D models were successfully constructed for all
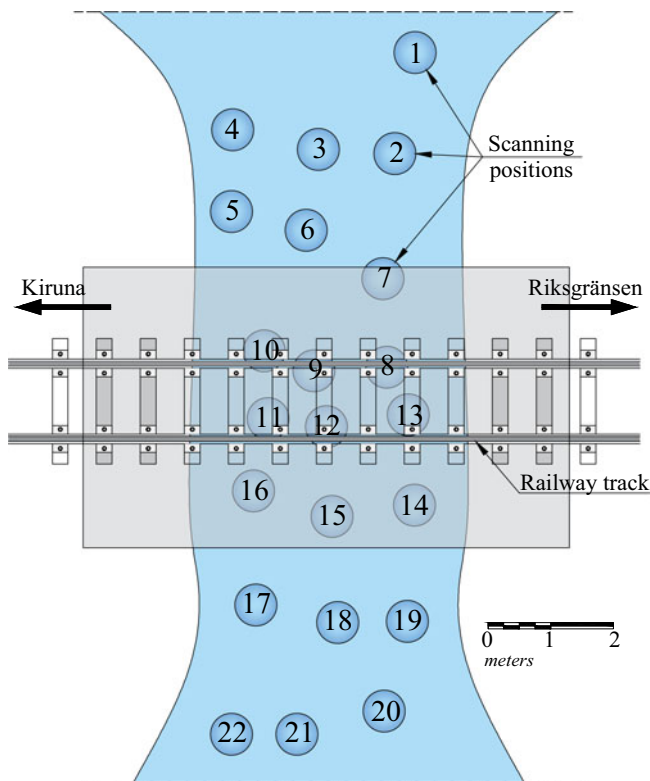
Figure 5. Scanning positions for the Juovajokk bridge (image based on data generated by Matterport app).

six bridges by TLS. These models included both the bridges' structural elements and secondary objects such as guardrails and surrounding vegetation. The point clouds obtained from TLS were grayscale, so no RGB information was available. The photogrammetry-based models also captured enough information to assess other objects of interest, such as the bridges' structural elements (abutments, piers, and the bridge deck). However, the only secondary elements that could be modeled were the guardrails; it was impossible to capture the vegetation surrounding the bridges because only ground-based photogrammetry was performed, limiting the size of the captured area.

Nevertheless, unlike the TLS models, the photogrammetry-based models included RGB data, allowing them to be visualised in a more natural way. The 3D models generated by IS captured less information than the models generated by TLS or photogrammetry. However, the abutments and bridge decks were captured with enough data to extract their general dimensions. Information about the bridge extremities, surrounding vegetation, and guardrails was not captured for any of the bridges because these elements were outside the Matterport camera's range. Like CRP, IS captured RGB data.

To investigate the influence of various factors on the quality of photogrammetric results, three different models were constructed for the Pahtajokk bridge based on the photos taken by Teams 1 and 2. This bridge was selected primarily because it was one of the last bridges to be scanned, so the less experienced Team 1 had acquired some confidence in using the equipment and performing the analyses (albeit not to the same level as Team 2) by the time

they worked on it. Factors whose influence were assessed included the experience of the team carrying out the scanning, the quality of image acquisition, and the analysts' post-processing skills and familiarity with the chosen software packages. In total, three photogrammetry-based models were created for Pahtajokk bridge:

- Model #1—Processing carried out by Team 1 using photos taken by Team 1 (Agisoft PhotoScan Pro + Canon 5D).
- Model #2—Processing carried out by Team 2 using photos taken by Team 1 (Bentley ContextCapture + Canon 5D).
- Model #3—Processing carried out by Team 2 using photos taken by Team 2 (Bentley ContextCapture + Canon 5D Mark II + 3DR Site Scan drone).

Model #2 was constructed by the experienced Team 2 using photos taken by the less experienced Team 1. The goal of the exercise was to identify factors that might hinder the creation of good quality 3D models. Such factors could include the quality of the photos (which may be limited by the camera's resolution, the degree of overlap, or the camera settings, among other things) and/or the analysts' skill at data processing and using the chosen software. Model #3 was based on both ground-based and aerial photogrammetry. This enabled the creation of a better model that benefited from the strengths of both approaches.

Ground-based photogrammetry can provide access to relatively narrow spaces where flying a drone might be problematic due to limited access, loss of (or weak) GPS signal, etc. Aerial photogrammetry allows the surroundings to be captured as well as the railway and top side of the bridge. For Model #3, the whole process (data acquisition and processing) was carried out by Team 2. Models #1, #2, and #3 are compared in Figure 11. Although both models are complete, some differences can be seen. Notably, there is a slight difference in contrast even though the models were created based on similar sets of photos. This is because Team 2 used a color calibration tool that can mimic the spectral reflectance of natural objects under various lighting conditions.

No other significant difference was found, demonstrating that the image quality and amount of overlap were sufficient to create the 3D models independently of the acquiring team's experience. This is important because the ease with which a new method can be adopted by inexperienced users (i.e. the steepness of its learning curve) will significantly affect its rate of uptake. Model #3 incorporated photographs taken using a drone, which enabled the entire area surrounding the bridge to be photographed. Differences in geometric accuracy between these models will be discussed in Section 6.2.

Another aspect worth comparing is the resolution offered by each method, which is a function of the point cloud density. This is an important factor because if the resolution is too low, it may be impossible to detect damage on the structural members. The abutment of Pahtajokk bridge was
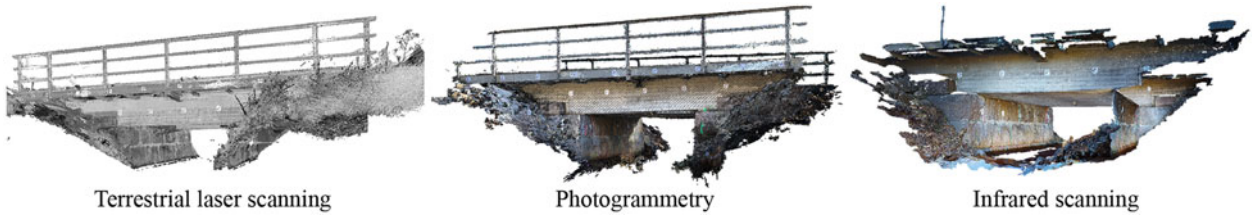
Terrestrial laser scanning   Photogrammetry   Infrared scanning

Figure 6. 3D models of Påunakbäcken bridge—differences in level of detail between the tested methods.

Terrestrial laser scanning   Photogrammetry   Infrared scanning

Figure 7. 3D models of Kedkejokk bridge—differences in level of detail between the tested methods.

Terrestrial laser scanning   Photogrammetry   Infrared scanning

Figure 8. 3D models of Juovajokk bridge—differences in level of detail between the tested methods.

Terrestrial laser scanning   Photogrammetry   Infrared scanning

Figure 9. 3D models of Pahtajokk bridge—differences in level of detail between the tested methods.

Terrestrial laser scanning   Photogrammetry   Infrared scanning

Figure 10. 3D models of Kallkällevägen bridge—differences in level of detail between the tested methods.
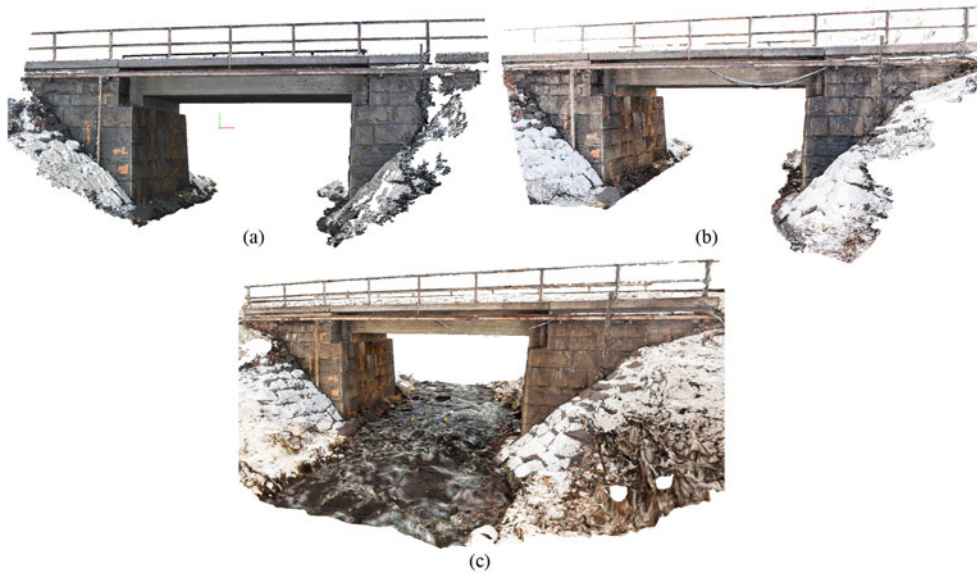
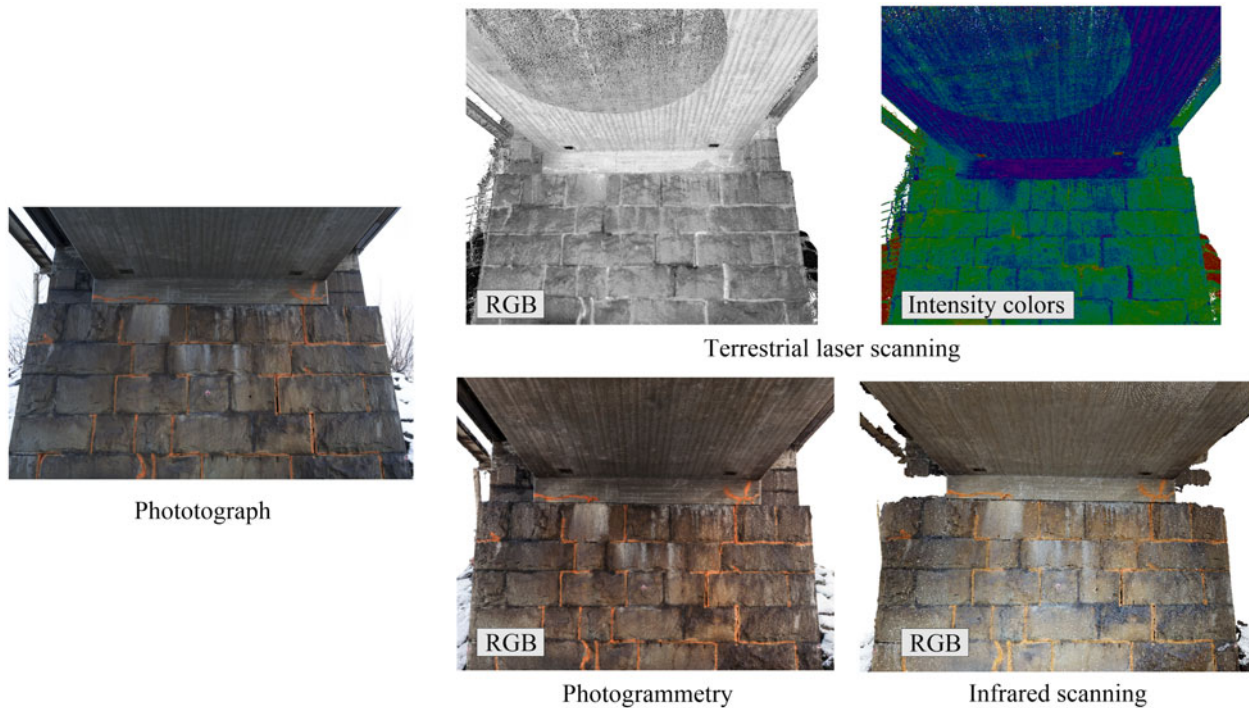**Figure 11.** CRP models of Pahtajokk bridge: (a) Model #1, (b) Model #2 and (c) Model #3.

Figure 12. Point cloud visualizations of the abutment of Pahtajokk bridge based on the TLS, CRP and IS models, with a field photograph for comparison.

selected because multiple joint dislocations were noticed during the field survey. Figure 12 compares the rendering capabilities of TLS, CRP, and IS to a field photograph, illustrating the differences in the methods' rendering capabilities. All three methods clearly achieve high levels of detail, although the IS model was less detailed than the TLS- and CRP-based models.

This was demonstrated by plotting the local densities of the point cloud of the same region shown in Figure 13. The TLS model achieved the highest estimated point cloud density, with an average density of about 228×10^3 points/m^2 (62,935 points/m^2 – standard deviation). The CRP model's density was similar (226×10^3 points/m^2 with 25229 points/

m^2 – standard deviation) but that of the IS model was appreciably lower (14×10^3 points/m^2 with 1643 points/m^2 – standard deviation). However, the IS and CRP models include RGB information that provides a more true-to-life image than can be generated using the intensity level scans provided by TLS.

6.2. Geometric deviations

The point clouds generated were imported into Autodesk ReCap to extract measurements. The "ground truth" for geometric measurements in remote sensing is nearly impossible to establish using devices such as a total station, which
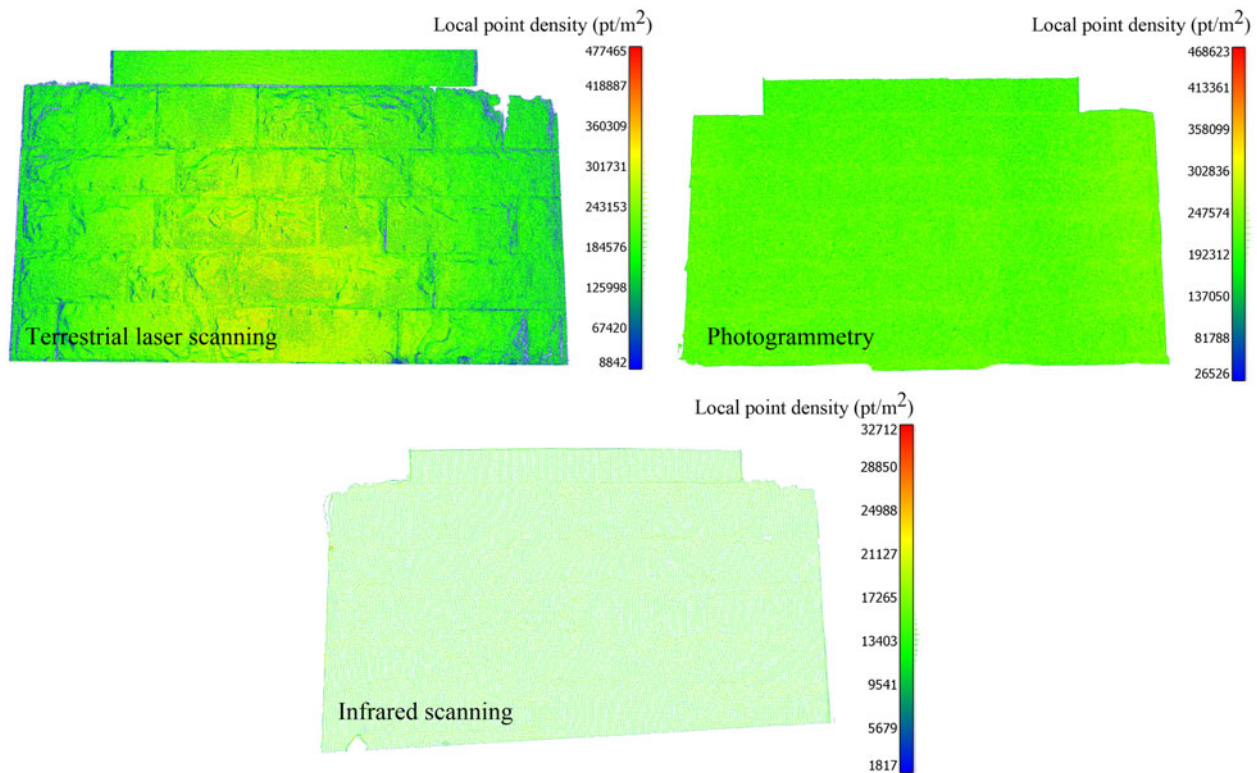
Figure 13. Local point cloud density for the region containing the abutment of the Pahjatokk bridge in the TLS, CRP and IS models.

itself may be prone to measurement error. Instead, the existing as-built drawings were used to establish the ground truth. The geometric deviations were analyzed based on point-wise measurements, but further studies would be helpful to compare the entire 3D models presented here to previously built models. This would enable the detection of global movements due to factors such as differential settlement that can induce torsional effects in the superstructure.

With a few exceptions, all methods provided good accuracy, as can be seen from Table 2. Because the Edbäcken bridge could not be recreated using the CRP and IS methods, no geometric deviations could be determined for this bridge. During the field trip, it was noticed that the Kedkejokk bridge had been repaired. The authors had no access to the updated drawings, so geometric deviations could not be computed for this bridge either. However, measurements are provided for comparison between the scanning techniques. If it is assumed that TLS provides measurements closest to reality, we can conclude that the IS data deviate only slightly whereas CRP had difficulties with scaling curved surfaces.

A comparison was also made between the different 3D models of the Pahtajokk bridge. Table 3, and the results presented in Figure 11 suggest that both teams performed the image acquisition process competently. However, there are significant differences in accuracy between Model #1 with Model #2, which were created using the same set of photos. The scanning of the Pahtajokk bridge was performed after a heavy snowfall, which created difficulties for Team 1 in attaching sufficient artificial targets. Consequently, the scaling was carried out with reduced redundancy. In their

workflow, Team 2 would provide a scale to the model based on the point cloud captured by TLS. This might be a reason for the large geometrical deviations; however, the analyst's processing skill, as well as the software capability, may also significantly affect model quality.

Figure 14 displays a qualitative comparison of imaging techniques used in this study in terms of cost, level of automation, accuracy/resolution, portability, range distance, and acquisition and processing time. Each method was given a grade of low, medium, or high for each item based on its performance, with the high grade corresponding to the best performance. For clarity, the high grade with respect to equipment cost was awarded to the method using the most affordable hardware; the high grade with respect to level of automation was awarded to methods with fully automatic data acquisition and processing; the high grade with respect to accuracy/resolution was awarded to the method with the highest accuracy and densest point cloud; the high grade with respect to portability was awarded to the method using the lightest and most flexible equipment; the high grade with respect to range was awarded to the method with the longest working range; and the high grade with respect to processing time was awarded to the method needing the least time for deployment, acquisition and processing.

For better interpretation a quantitative comparison in terms of actual equipment, data acquisition and processing time, will be provided in the following. The equipment costs can be approximated to about 50,000 € for TLS, 1400 € for CRP, and 4700 € for IS. Data acquisition varies based on the size and ease of movement around scanned bridges, from the authors' experience with studied bridges the TLS

Table 2. TLS, CRP and IS accuracy comparison.

Bridge	As-built dimension (mm)	Terrestrial laser scanning		Close-range photogrammetry		Infrared scanning	
		(mm)	%ΔL	(mm)	%ΔL	(mm)	%ΔL
Edbäcken bridge							
Span	5800	5724	−1.31%	–	–	–	–
Width (deck)	3800	3882	2.16%	–	–	–	–
Påunakbäcken bridge							
Span	2950	2930	−0.68%	2947	−0.10%	2985	1.19%
Width (deck)	4500	4517	0.38%	4525	0.56%	4546	1.02%
Kedkejokk bridge							
Span	4000[a]	2750	–	3080	–	2727	–
Rise	2000[a]	1353	–	1540	–	1286	–
Juovajokk bridge							
Span	5500	5434	−1.20%	5412	−1.60%	5458	−0.76%
Width (deck)	3800	3780	−0.53%	3735	−1.71%	3780	−0.53%
Pahtajokk bridge							
Span	6900	6928	0.41%	7735	12.10%	6958	0.84%
Width (deck)	3900	3904	0.10%	4376	12.21%	3926	0.67%
Kallkällevägen bridge							
Central span (interax)	14,500	14,592	0.63%	14468	−0.22%	14828	2.26%
Width (deck)	4540	4526	−0.31%	4510	−0.66%	4628	1.94%
Diameter (pillar)	1000	1000	0.00%	977	−2.30%	1009	0.90%

[a]Original values before repair.

Table 3. Comparison between different CRP-based models of Pahtajokk bridge.

Bridge	TLS (mm)	Photogrammetry 3D model #1		Photogrammetry 3D model #2		Photogrammetry 3D model #3	
		(mm)	%ΔL	(mm)	%ΔL	(mm)	%ΔL
Pahtajokk bridge							
Span	6928	7735	11.65%	6836	−1.33%	6832	−1.38%
Width (deck)	3904	4376	12,09%	3854	−1.28%	3897	−0.18%

3D model #1—Processing by Team 1 with photos taken by Team 1 (Agisoft PhotoScan Pro + Canon 5D). 3D model #2—Processing by Team 2 with photos taken by Team 1 (Bentley ContextCapture + Canon 5D). 3D model #3—Processing by Team 2 with photos taken by Team 2 (Bentley ContextCapture + Canon 5D Mark II).
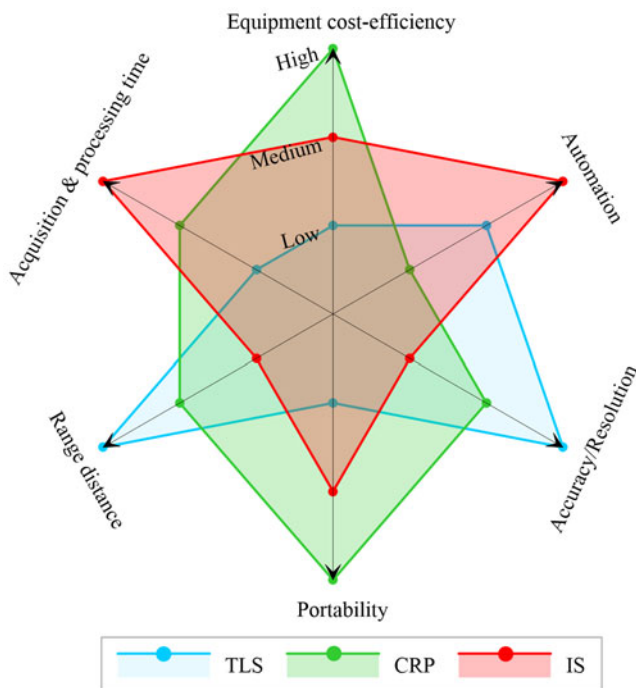

Figure 14. Performance of the 3D imaging methods (the *high* level represents the best performance with respect to the indicated item).

would be completed in about 1–2 hours, CRP in about 1–4 hours, while IS in about 15 min–2 h. The postprocessing time could take up to 7 days for both TLS and CRP (including computational time/point cloud registration and final cleaning of irrelevant points), and 2 days for IS.

7. Conclusions

This study investigated the use of three optical methods for creating digital models of bridges. It has been shown that the 3D models could serve as a tool for bridge inspectors from which measurements could be extracted. A full off-site inspection is currently not feasible as some areas of the bridges were difficult to capture mainly due to restricted access and narrow spaces. Although promising, attempting to virtually duplicate the bridge and its close environment was not without some merit. The 3D models created would enable a preliminary inspection without the need for lengthy journeys to distant bridges. Once the data is gathered by a technician, the 3D model can be made available to all stakeholders (bridge managers, NDT technicians, structural engineers, etc.) to make their own judgments regarding the scanned object and plan for further and more in-depth assessment activities. The methods presented are only providing near-surface information, and therefore, in-depth inspection should not be overlooked. The difficulty to capture local defects such as delaminations and narrow cracks also reduces versatility.

The tested methods employed were terrestrial laser scanning (TLS), close-range photogrammetry (CRP), and

infrared scanning (IS). Each method was applied to six concrete railway bridges. The main conclusions were:

- All methods produced digital models with different levels of completeness, from which general measurements (span lengths, deck widths, vertical underclearance, pier diameters, etc.) could be extracted with good accuracy.
- The point clouds generated by TLS and CRP were much denser than those generated by IS. Denser point clouds enable better visualization at the cost of increased computational time and storage requirements, as well as greater difficulties in handling the models.
- The CRP and IS methods produced RGB data whereas TLS produced only intensity data. RGB data yields more true-to-life images, which may help inspectors to detect damage.
- No special training is needed to create good quality 3D models using CRP or IS imaging. However, a high level of processing skill and familiarity with the processing software can appreciably increase the accuracy of the models generated by CRP. The IS method is highly automated, which is beneficial in many respects but reduces the bridge inspector's control and the scope for improving the final model. The IS method appears to have considerable potential provided that further improvements are made in cloud computing solutions and range.
- The 3D models can be improved by combining ground-based and aerial photogrammetry, which makes it possible to capture both primary (the bridge itself) and secondary elements that may warrant investigation (e.g. vegetation and, proximity access etc.).

Despite some drawbacks, 3D imaging technologies have many advantages that make them increasingly attractive to transport agencies. The use of remote and contactless technology to improve assessment procedures could significantly reduce track possession, avoid traffic delays and ultimately ensure people's safety. These methods would also help to improve the accuracy and efficiency of bridge inspections by eliminating human error, and provide opportunities to create historical records of the progress of deterioration. Beneficial future developments could include automated damage detection using artificial intelligence, and methods for enriching 3D models by incorporating additional information on variables such as material properties and inner geometry (reinforcement). Such enhanced 3D models would facilitate interpretation, analysis and data sharing between all stakeholders, including NDT technicians, bridge engineers and bridge managers.

Acknowledgments

ORCID

Cosmin Popescu 🇫 http://orcid.org/0000-0001-9423-7436
Lennart Elfgren 🇫 http://orcid.org/0000-0002-0560-9355

References

Abdelbarr, M., Chen, Y. L., Jahanshahi, M. R., Masri, S. F., Shen, W.-M., & Qidwai, U. A. (2017). 3D dynamic displacement-field measurement for structural health monitoring using inexpensive RGB-D based sensor. *Smart Materials and Structures*, *26*(12), 125016. doi:10.1088/1361-665X/aa9450

Abu Dabous, S., Yaghi, S., Alkass, S., & Moselhi, O. (2017). Concrete bridge deck condition assessment using IR thermography and ground penetrating radar technologies. *Automation in Construction*, *81*, 340–354. doi:10.1016/j.autcon.2017.04.006

Alani, A. M., Aboutalebi, M., & Kilic, G. (2014). Integrated health assessment strategy using NDT for reinforced concrete bridges. *NDT & E International*, *61*, 80–94. doi:10.1016/j.ndteint.2013.10.001

Baqersad, J., Poozesh, P., Niezrecki, C., & Avitabile, P. (2017). Photogrammetry and optical methods in structural dynamics – A review. *Mechanical Systems and Signal Processing*, *86*, 17–34. doi:10.1016/j.ymssp.2016.02.011

Bentley. (2018). ContextCapture - 3D reality modelling software. Retrieved from https://www.bentley.com/en/products/brands/contextcapture.

Bhatla, A., Choe, S. Y., Fierro, O., & Leite, F. (2012). Evaluation of accuracy of as-built 3D modeling from photos taken by handheld digital cameras. *Automation in Construction*, *28*, 116–127. doi:10.1016/j.autcon.2012.06.003

Chen, S.-E., Liu, W., Bian, H., & Smith, B. (2012). 3D LiDAR scans for bridge damage evaluations. *Forensic Engineering*, *2012*, 487–495.

Conde, B., Ramos, L. F., Oliveira, D. V., Riveiro, B., & Solla, M. (2017). Structural assessment of masonry arch bridges by combination of non-destructive testing techniques and three-dimensional numerical modelling: Application to Vilanova bridge. *Engineering Structures*, *148*, 621–638. doi:10.1016/j.engstruct.2017.07.011

Cultural Heritage Imaging. (2018). Photogrammetry - How to capture photos. Retrieved from http://culturalheritageimaging.org/Technologies/Photogrammetry/#how_to.

Duque, L., Seo, J., & Wacker, J. (2018). Synthesis of unmanned aerial vehicle applications for infrastructures. *Journal of Performance of Constructed Facilities*, *32*(4), 04018046. doi:10.1061/(ASCE)CF.1943-5509.0001185

Fathi, H., & Brilakis, I. (2011). Automated sparse 3D point cloud generation of infrastructure using its distinctive visual features. *Advanced Engineering Informatics*, *25*(4), 760–770. doi:10.1016/j.aei.2011.06.001

Franco, J. M., Mayag, B. M., Marulanda, J., & Thomson, P. (2017). Static and dynamic displacement measurements of structural elements using low cost RGB-D cameras. *Engineering Structures*, *153*, 97–105. doi:10.1016/j.engstruct.2017.10.018

Fritsch, D., & Klein, M. (2018). 3D preservation of buildings – Reconstructing the past. *Multimedia Tools and Applications*, *77*(7), 9153–9170. doi:10.1007/s11042-017-4654-5

Golparvar-Fard, M., Bohn, J., Teizer, J., Savarese, S., & Peña-Mora, F. (2011). Evaluation of image-based modeling and laser scanning accuracy for emerging automated performance monitoring techniques. *Automation in Construction*, 20(8), 1143–1155. doi:10.1016/j.autcon.2011.04.016

Graybeal, B. A., Phares, B. M., Rolander, D. D., Moore, M., & Washer, G. (2002). Visual inspection of highway bridges. *Journal of Nondestructive Evaluation*, 21(3), 67–83. doi:10.1023/A:1022508121821

Henry, P., Krainin, M., Herbst, E., Ren, X., & Fox, D. (2014). RGB-D mapping: Using depth cameras for dense 3D modeling of indoor environments. In O. Khatib, V. Kumar, and G. Sukhatme (Eds.), *Experimental robotics: The 12th international symposium on experimental robotics* (pp. 477–491). Berlin: Springer Berlin Heidelberg.

Hess, M., Petrovic, V., Yeager, M., & Kuester, F. (2018). Terrestrial laser scanning for the comprehensive structural health assessment of the Baptistery di San Giovanni in Florence, Italy: An integrative methodology for repeatable data acquisition, visualization and analysis. *Structure and Infrastructure Engineering*, 14(2), 247–263. doi:10.1080/15732479.2017.1349810

Hugenschmidt, J. (2002). Concrete bridge inspection with a mobile GPR system. *Construction Building Materials*, 16(3), 147–154. doi:10.1016/S0950-0618(02)00015-6

Jáuregui, D., Tian, Y., & Jiang, R. (2006). Photogrammetry applications in routine bridge inspection and historic bridge documentation. *Transportation Research Record: Journal of the Transportation Research Board*, 1958(1), 24–32. doi:10.1177/0361198106195800103

Jáuregui, D. V., White, K. R., Pate, J. W., & Woodward, C. B. (2005). Documentation of bridge inspection projects using virtual reality approach. *Journal of Infrastructure Systems*, 11(3), 172–179. doi:10.1061/(ASCE)1076-0342(2005)11:3(172)

Jáuregui, D. V., White, K. R., Woodward, C. B., & Leitch, K. R. (2003). Noncontact photogrammetric measurement of vertical bridge deflection. *Journal of Bridge Engineering*, 8(4), 212–222. doi:10.1061/(ASCE)1084-0702(2003)8:4(212)

Jiménez, A., & Gärdin, D. C. (2018). *Optical methods for 3D-reconstruction of railway bridges: Infrared scanning*, close range photogrammetry and Terrestrial laser scanning (MSc thesis). Luleå University of Technology, Luleå.

Khaloo, A., Lattanzi, D., Cunningham, K., Dell'Andrea, R., & Riley, M. (2018). Unmanned aerial vehicle inspection of the Placer River Trail Bridge through image-based 3D modelling. *Structure and Infrastructure Engineering*, 14(1), 124–136. doi:10.1080/15732479.2017.1330891

Liu, W., Chen, S. E., Boyajian, D., & Hauser, E. (2010). Application of 3D LIDAR scan of a bridge under static load testing. *Materials Evaluation*, 68(12), 1359–1367.

Liu, W., Chen, S-e., & Hasuer, E. (2012). Bridge clearance evaluation based on terrestrial LIDAR scan. *Journal of Performance of Constructed Facilities*, 26(4), 469–477. doi:10.1061/(ASCE)CF.1943-5509.0000208

LLC, A. (2017). *Agisoft PhotoScan – Fully automated professional photogrammetric kit*. St. Petersburg: Agisoft PhotoScan.

Miranda, F., & Abreu, C. (2016). *Handbook of research on computational simulation and modeling in engineering*. Hershey, PA: IGI Global.

Omar, T., & Nehdi, M. L. (2017). Remote sensing of concrete bridge decks using unmanned aerial vehicle infrared thermography. *Automation in Construction*, 83, 360–371. doi:10.1016/j.autcon.2017.06.024

Phares, B. M., Washer, G. A., Rolander, D. D., Graybeal, B. A., & Moore, M. (2004). Routine highway bridge inspection condition documentation accuracy and reliability. *Journal of Bridge Engineering*, 9(4), 403–413. doi:10.1061/(ASCE)1084-0702(2004)9:4(403)

Riveiro, B., González-Jorge, H., Varela, M., & Jauregui, D. V. (2013). Validation of terrestrial laser scanning and photogrammetry techniques for the measurement of vertical underclearance and beam geometry in structural inspection of bridges. *Measurement*, 46(1), 784–794. doi:10.1016/j.measurement.2012.09.018

Riveiro, B., Jauregui, D. V., Arias, P., Armesto, J., & Jiang, R. (2012). An innovative method for remote measurement of minimum vertical underclearance in routine bridge inspection. *Automation in Construction*, 25, 34–40. doi:10.1016/j.autcon.2012.04.008

Riveiro, B., & Solla, M. (2016). *Non-destructive techniques for the evaluation of structures and infrastructure*. London: CRC Press.

Stavroulaki, M. E., Riveiro, B., Drosopoulos, G. A., Solla, M., Koutsianitis, P., & Stavroulakis, G. E. (2016). Modelling and strength evaluation of masonry bridges using terrestrial photogrammetry and finite elements. *Advances in Engineering Software*, 101, 136–148. doi:10.1016/j.advengsoft.2015.12.007

Takimoto, R. Y., Tsuzuki, M. D S. G., Vogelaar, R., Martins, T. D C., Sato, A. K., Iwao, Y., Gotoh, T., & Kagei, S. (2016). 3D reconstruction and multiple point cloud registration using a low precision RGB-D sensor. *Mechatronics*, 35, 11–22. doi:10.1016/j.mechatronics.2015.10.014

Vaghefi, K., Ahlborn, T. M., Harris, D. K., & Brooks, C. N. (2015). Combined imaging technologies for concrete bridge deck condition assessment. *Journal of Performance of Constructed Facilities*, 29(4), 04014102. doi:10.1061/(ASCE)CF.1943-5509.0000465

Vaghefi, K., Oats, R. C., Harris, D. K., Ahlborn, T. M., Brooks, C. N., Endsley, K. A., Roussi, C., Shuchman, R., Burns, J. W., & Dobson, R. (2012). Evaluation of commercially available remote sensors for highway bridge condition assessment. *Journal of Bridge Engineering*, 17(6), 886–895. doi:10.1061/(ASCE)BE.1943-5592.0000303

Watson, C., Chen, S.-E., Bian, H., & Hauser, E. (2012). Three-dimensional terrestrial LIDAR for operational bridge clearance measurements. *Journal of Performance of Constructed Facilities*, 26(6), 803–811. doi:10.1061/(ASCE)CF.1943-5509.0000277

Weinmann, M. (2016). *Reconstruction and analysis of 3D scenes*. New York, NY: Springer International Publishing. doi:10.1007/978-3-319-29246-5